

Parameter Estimation of Hybrid Sinusoidal FM-Polynomial Phase Signal

Wang, Pu; Orlik, Philip V.; Sadamoto, Kota; Tsujita, Wataru

TR2016-158 December 19, 2016

Abstract

This paper considers parameter estimation of a hybrid sinusoidal frequency modulated (FM) and polynomial phase signal (PPS) from a limited number of samples. We first show limitations of an existing method, the high-order ambiguity function (HAF), and then propose a new method by adopting the high-order phase function which was originally designed for the pure PPS. The proposed method estimates parameters of interest from peak locations in the time-frequency rate domain, which are less perturbed by the noise than peak values used by the HAF-based method. Numerical evaluation shows, the proposed method can handle the hybrid FM-PPS signal with low sinusoidal frequency and improve estimation accuracy in terms of mean squared error for several orders of magnitude.

IEEE Signal Processing Letters

© 2016 MERL. This work may not be copied or reproduced in whole or in part for any commercial purpose. Permission to copy in whole or in part without payment of fee is granted for nonprofit educational and research purposes provided that all such whole or partial copies include the following: a notice that such copying is by permission of Mitsubishi Electric Research Laboratories, Inc.; an acknowledgment of the authors and individual contributions to the work; and all applicable portions of the copyright notice. Copying, reproduction, or republishing for any other purpose shall require a license with payment of fee to Mitsubishi Electric Research Laboratories, Inc. All rights reserved.

Parameter Estimation of Hybrid Sinusoidal FM-Polynomial Phase Signal

Pu Wang, Philip V. Orlik, Kota Sadamoto, Wataru Tsujita, and Fulvio Gini, *Fellow, IEEE*

Abstract—This paper considers parameter estimation of a hybrid sinusoidal frequency modulated (FM) and polynomial phase signal (PPS) from a limited number of samples. We first show limitations of an existing method, the high-order ambiguity function (HAF), and then propose a new method by adopting the high-order phase function which was originally designed for the pure PPS. The proposed method estimates parameters of interest from *peak locations* in the time-frequency rate domain, which are less perturbed by the noise than *peak values* used by the HAF-based method. Numerical evaluation shows, the proposed method can handle the hybrid FM-PPS signal with low sinusoidal frequency and improve estimation accuracy in terms of mean squared error for several orders of magnitude.

Index Terms—Parameter estimation, frequency modulation, polynomial phase signal, high-order phase function.

I. INTRODUCTION

Parameter estimation of polynomial phase signals (PPSs) from a finite number of samples is a fundamental problem in many applications, including radar, sonar, communications, acoustics and optics [1]–[11]. In this paper, we consider a special PPS model: a hybrid sinusoidal frequency modulated (FM) and PPS signal (referred to as the hybrid sinusoidal FM-PPS),

$$\begin{aligned} y(n) &= x(n) + v(n), \quad n = 0, 1, \dots, N-1, \\ &= Ae^{j2\pi b \sin(2\pi f_0 n + \phi_0)} e^{j2\pi \sum_{p=0}^P a_p n^p / p!} + v(n) \end{aligned} \quad (1)$$

where A is the unknown amplitude, $b > 0$ is the sinusoidal FM modulation index, f_0 is the sinusoidal FM frequency, ϕ_0 is the initial phase, $\{a_p\}_{p=0}^P$ are the PPS phase parameters, P is the polynomial order, $v(n)$ is the white Gaussian noise with an unknown variance σ^2 , N is the number of samples.

Compared with the vast literature on the pure PPS signal [1]–[11], the hybrid sinusoidal FM-PPS of (1) receives less attention [12]–[17]. As pointed out in [17], one primary motivation to study the hybrid FM-PPS comes from Doppler radar systems. On one hand, when a target is moving at a time-varying acceleration, outputs at the matched filter can be

modeled as a pure PPS with the phase parameter $\{a_p\}_{p=0}^P$ associated to the kinematic parameters of the moving target. For instance, the initial velocity and acceleration are proportional to a_1 and a_2 , respectively. On the other hand, rotating parts (e.g., rotating blades of a helicopter) and target vibration (e.g., jet engine) introduce the sinusoidal FM component [12]–[15]. With both effects, the matched filter outputs follow the hybrid signal model in (1).

In this paper, we are still interested in the parameter estimation of the hybrid sinusoidal FM-PPS of (1), but focus on applications where a low sinusoidal FM frequency f_0 is often observed. We first show limitations of an existing method, the high-order ambiguity function (HAF), especially when f_0 is relatively small, and then propose a new approach which makes use of the high-order phase function (HPF), originally designed for the pure PPS, and locally approximates the sinusoidal FM component in the nonlinear kernel by a second-order Taylor series expansion. We discuss how to determine the local region (over the delay) to make the Taylor expansion error less than a given threshold. Finally, the proposed method is numerically compared to competing methods in terms of identifiability, computational complexity and estimation accuracy.

II. PRIOR ARTS

We start with a brief review of existing methods for the parameter estimation of the signal in (1). The optimal maximum likelihood (ML) estimation minimizes the negative log-likelihood function [18] which is known to yield a multi-dimensional search and, hence, is computationally prohibited from practical applications.

A computational efficient estimator is based on phase unwrapping (PU) followed by a nonlinear least square (NLS) fitting, referred to the PULS method here. Denote $\hat{\phi}(n)$ the unwrapped phase, the PULS method minimizes the function

$$\min_{b, f_0, \phi_0, a_p} \sum_{n=0}^{N-1} \left| \frac{\hat{\phi}(n)}{2\pi} - b \sin(2\pi f_0 n + \phi_0) - \sum_{p=0}^P \frac{a_p n^p}{p!} \right|^2 \quad (2)$$

where the estimation of f_0 involves a one-dimensional search. Although computationally simple, this approach may show limited performance at low signal-to-noise ratios (SNRs) due to the phase unwrapping step. In addition, the PULS method cannot be applied to the multi-component scenario.

Proposed for the pure PPS and as a non-parametric estimator [19], [20], the quasi maximum likelihood (QML) method can be extended for the hybrid FM-PPS. It fits the instantaneous frequency (IF) extracted by the short-time Fourier transform

Copyright (c) 2015 IEEE. Personal use of this material is permitted. However, permission to use this material for any other purposes must be obtained from the IEEE by sending a request to pubs-permissions@ieee.org.

P. Wang and P. V. Orlik are with Mitsubishi Electric Research Laboratories (MERL), 201 Broadway, Cambridge, MA 02139, USA (e-mail: {pwang, porlik}@merl.com).

K. Sadamoto and W. Tsujita are with Mitsubishi Electric Advanced Technology R&D Center, Amagasaki City, 661-8661, Japan (e-mail: sadamoto.kota@ea.mitsubishielectric.co.jp, tsujita.wataru@eb.mitsubishielectric.co.jp).

F. Gini is with the Department of Ingegneria dell'Informazione, University of Pisa, Pisa, Italy (e-mail: f.gini@ing.unipi.it).

(STFT) with the NLS (similar to (2)). Since the STFT gives biased estimates of the IF, the above process has to be repeated over a set of STFT window sizes and the one giving the maximum estimated likelihood is chosen. With an additional refining step [21], the QML method further reduces the bias and show low SNR threshold. However, due to the iterative process, its complexity may be still too high for certain applications.

The HAF method, originally designed for the pure PPS [3], [5], was particularly designed to jointly estimate the hybrid sinusoidal FM-PPS in [17]. Specifically, the HAF computes a high-order nonlinear kernel

$$s_1(n) = y(n), \quad s_2(n; \tau_1) = y(n + \tau_1)y^*(n - \tau_1), \quad (3)$$

$$s_M(n; \tau_{M-1}) = s_{M-1}(n + \tau_{M-1}; \tau_{M-2})s_{M-1}^*(n - \tau_{M-1}; \tau_{M-2})$$

where $\tau_M = [\tau_1, \dots, \tau_M]$ groups all delay coefficients. Plugging (1) into (3) results in

$$s_M(n; \tau_{M-1}) = A_M e^{j[\omega_c n + \psi_c + \beta \sin(2\pi f_0 n + \psi_0)]}, \quad (4)$$

where $A_M = |A|^{2^{M-1}}$, $\omega_c = 2^M \pi a_M Q_\tau$, $\psi_c = 2^M \pi a_{M-1} Q_\tau$, $\beta = 2^M \pi b \prod_{m=1}^{M-1} \sin(2\pi f_0 \tau_m)$ and $\psi_0 = \phi_0 + (M-1)\pi/2$ with $Q_\tau = \prod_{m=1}^{M-1} \tau_m$. It is seen from (4) that this nonlinear kernel generates a single-tone FM signal with a tone frequency at ω_c and a sinusoidal FM frequency at $2\pi f_0$. In [17], this single-tone FM signal is approximated by a superposition of multiple harmonics

$$s_M(n; \tau_{M-1}) \approx A_M \sum_{k=-K}^K J_k(\beta) e^{j[(\omega_c + 2\pi f_0 k)n + \psi_c + k\psi_0]} \quad (5)$$

where K is the maximum order of the Bessel function of the first kind $J_k(\cdot)$. (5) implies that the single-tone FM signal can be decomposed into $(2K+1)$ harmonics with the tone frequency sweeping from $\omega_c - 2\pi K f_0$ to $\omega_c + 2\pi K f_0$ at an inter-peak stepsize $2\pi f_0$. As a result, one can estimate f_0 and a_M (via ω_c) by identifying the $(2K+1)$ peak locations of the FFT spectrum of $s_M(n; \tau_{M-1})$. The estimation of β can be obtained from the peak values $J_k(\beta)$.

Although the HAF-based method shows advantages over the phase unwrapping method [17], it may have several issues. First, it may not be an easy task to correctly identify multiple local peaks (see the following Fig. 1). Second, the use of *peak values* to estimate the sinusoidal FM index b may result in larger estimation errors (also noted in Examples 1 and 2 of [17]). Third, the HAF may fail to handle the hybrid FM-PPS signal when the sinusoidal FM frequency f_0 is small, a particular scenario of our interest. This is due to the FFT spectrum resolution which is determined by $1/N$. To identify these $(2k+1)$ peaks, the inter-peak distance of f_0 has to be at least $1/N$, i.e., $f_0 \geq 1/N$. When f_0 is small, the HAF spectra cannot resolve these $(2K+1)$ peaks. For example, we consider the same hybrid FM-PPS with $P=2$ in *Example 2* of [17] with parameters $A=1$, $b=6$, $\phi_0=0$, $a_0=0.5$, $a_1=0.1$, $a_2=3.4722 \cdot 10^{-4}$, $N=1024$, and $\omega_0=2\pi f_0=0.0491$. The top plots of Fig. 1 show that the HAF-based method with $\tau = \{32, 129\}$ is able to form multiple peaks which align with the analytical locations of $\{\omega_c + 2\pi f_0 k\}_{k=-K}^K$ (denoted as vertical red lines and $K=3$). Specifically, the HAF spectra

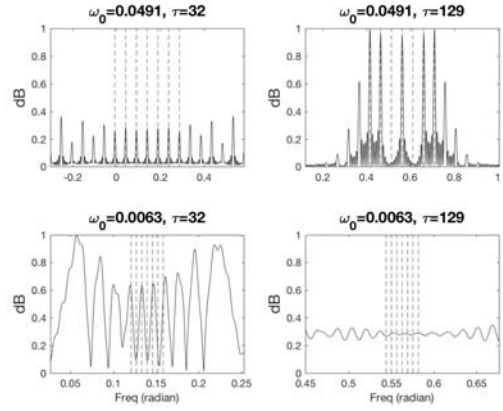


Fig. 1. The HAF spectra of the hybrid FM-PPS with $P=2$ in the noise-free case. Vertical red lines denote the analytical peaks at $\{\omega_c + 2\pi f_0 k\}_{k=-K}^K$ with $K=3$. Top row: $\omega_0 = 2\pi f_0 = 0.0491$, the same case as *Example 2* of [17]; Bottom row: $\omega_0 = 2\pi f_0 = 0.0063$, a resolution issue.

with $\tau = 129$ gives the same result shown in Fig. 1 (b) of [17]. Next, we change the sinusoidal FM frequency to $\omega_0 = 2\pi f_0 = 0.0063$. As shown in the bottom plots of Fig. 1, the HAF-based method is no longer able to resolve multiple peaks as the FFT resolution cannot support the finer separation of peaks separated by f_0 .

III. PROPOSED ESTIMATOR

In this section, we first introduce another nonlinear kernel of HPF, originally designed for pure PPS [7], [9], and propose a local version of the HPF for the hybrid FM-PPS.

A. High-order Phase Function

The HPF employs the following nonlinear transform [7], [9]

$$c_L(n; \mathbf{d}, \mathbf{r}) = \prod_{l=1}^L [y(n + d_l \tau) y(n - d_l \tau)]^{r_l}, \quad (6)$$

where $\mathbf{d} = [d_1, \dots, d_L]$, $\mathbf{r} = [r_1, \dots, r_L]$, $[\cdot]^{r_l}$ denotes the conjugation if $r_l = -1$, and $\tau \in \Gamma(n)$ with $\Gamma(n)$ denoting the feasible range of τ at time n . For a pure PPS, the HPF selects the coefficients \mathbf{d} and \mathbf{r} such as $\sum_{l=1}^L r_l d_l^2 = 1$ and $\sum_{l=1}^L r_l d_l^m = 0$ for even values of $4 \leq m \leq P$ [9, Proposition 1], and integrates the nonlinear kernel along τ^2 ,

$$H_L(n, \Psi) = \sum_{\tau \in \Gamma(n)} c_L(n; \mathbf{d}, \mathbf{r}) e^{-j2\pi \Psi \tau^2}, \quad (7)$$

where Ψ is the index for the instantaneous frequency rate (IFR), i.e., the second-order phase derivative. It can be shown that, for any given time n , the squared magnitude of $H_L(n, \Psi)$ is centered on $\text{IFR}(n) = \sum_{p=2}^{P-2} a_p n^{p-2} / (p-2)!$ due to the match filtering in (7).

B. The Proposed Estimator

For the hybrid signal in (1), the nonlinear kernel of (6) gives

$$c_L(n; \mathbf{d}, \mathbf{r}) = A^{2L} e^{j2\pi \varphi} e^{j2\pi \text{IFR}(n) \tau^2} e^{j4\pi b \sin(2\pi f_0 n + \phi_0) \sum_{l=1}^L r_l \cos(2\pi f_0 d_l \tau)}. \quad (8)$$

It is seen that the first two exponential terms are related to the PPS component with φ independent of τ and $\text{IFR}(n)$

associated with τ^2 . The last exponential term is from the sinusoidal FM component and is nonlinear (via $\cos(\cdot)$) over τ . Therefore, directly integrating $c_L(n; \mathbf{d}, \mathbf{r})$ over $\tau \in \Gamma(n)$ cannot coherently accumulate the signal energy along τ^2 .

To coherently integrate the kernel over τ^2 , we locally approximate $\cos(2\pi f_0 d_l \tau)$ by its Taylor series expansion, i.e.,

$$\cos(2\pi f_0 d_l \tau) \approx 1 - \frac{(2\pi f_0)^2 \tau^2}{2} d_l^2, \quad |\tau| \leq \epsilon \quad (9)$$

where ϵ defines a local region around $\tau = 0$. With (9), the local kernel of (8) is given as

$$\tilde{c}_L(n; \mathbf{d}, \mathbf{r}) = A^{2L} e^{j2\pi\varphi} e^{j4\pi b \sin(2\pi f_0 n + \phi_0)} \sum_{l=1}^L r_l \quad (10)$$

$$e^{j2\pi[\text{IFR}(n) - b \sin(2\pi f_0 n + \phi_0)](2\pi f_0)^2 \tau^2}, \quad |\tau| \leq \epsilon,$$

where we have used the fact that $\sum_{l=1}^L r_l d_l^2 = 1$. Then the local HPF integrates the local kernel over $-\epsilon \leq \tau \leq \epsilon$

$$\tilde{H}_L(n, \Psi) = \sum_{\tau=-\epsilon}^{\epsilon} \tilde{c}_L(n; \mathbf{d}, \mathbf{r}) e^{-j2\pi\Psi\tau^2}, \quad (11)$$

which achieves the maxima along the trajectory

$$\Psi(n) = \sum_{p=2}^P \frac{a_p n^{p-2}}{(p-2)!} - 4\pi^2 f_0^2 b \sin(2\pi f_0 n + \phi_0). \quad (12)$$

It is seen that the local HPF embeds the parameters of interest ($\{a_p\}_{p=2}^P, b, f_0, \phi_0$) into peak locations. For the pure PPS, i.e., $b = 0$, the local HPF forms the peak ridge along its IFR(n).

C. Parameter Estimation

From (12), we can extract the peak locations and estimate these parameters by the following steps. First, group K peak locations $\hat{\Psi} = [\hat{\Psi}(n_0), \dots, \hat{\Psi}(n_0 + K - 1)]^T$, construct the matrix $\mathbf{H}(f) = [\mathbf{n}_2, \dots, \mathbf{n}_P, \mathbf{s}(f), \mathbf{c}(f)]$ with columns given as

$$\mathbf{n}_p = [n_0^{p-2}/(p-2)!, \dots, n_{n_0+K-1}^{p-2}/(p-2)!]^T,$$

$$\mathbf{s}(f) = [\sin(2\pi f n_0), \dots, \sin(2\pi f(n_0 + K - 1))]^T,$$

$$\mathbf{c}(f) = [\cos(2\pi f n_0), \dots, \cos(2\pi f(n_0 + K - 1))]^T, \quad (13)$$

and solve the following least square problem

$$\hat{f}_0 = \min_f \|\hat{\Psi} - \mathbf{H}(f)\mathbf{g}\|^2 = \min_f \hat{\Psi}^T \mathbf{P}_{\mathbf{H}(f)}^\perp \hat{\Psi} \quad (14)$$

where \mathbf{g} is a $(P+1) \times 1$ linear parameter vector and $\mathbf{P}_{\mathbf{H}(f)}^\perp = \mathbf{I} - \mathbf{H}(f)(\mathbf{H}^T(f)\mathbf{H}(f))^{-1}\mathbf{H}^T(f)$ is the projection matrix. With the estimated \hat{f}_0 , we have

$$\hat{\mathbf{g}} = \left(\mathbf{H}^T(\hat{f}_0)\mathbf{H}(\hat{f}_0) \right)^{-1} \mathbf{H}^T(\hat{f}_0)\hat{\Psi}. \quad (15)$$

Then the remaining $(P+1)$ parameters can be estimated as

$$\hat{a}_2 = \hat{\mathbf{g}}(1), \dots, \hat{a}_P = \hat{\mathbf{g}}(P-1), \quad (16)$$

$$\hat{b} = \frac{\sqrt{\hat{\mathbf{g}}^2(P) + \hat{\mathbf{g}}^2(P+1)}}{4\pi^2 \hat{f}_0^2}, \quad \hat{\phi}_0 = \arctan\left(\frac{\hat{\mathbf{g}}(P+1)}{\hat{\mathbf{g}}(P)}\right).$$

With the above estimated parameters, we can demodulate the original signal as $\hat{y}(n) = y(n)e^{-j2\pi b \sin(2\pi f_0 n + \phi_0)} e^{-j2\pi \sum_{p=2}^P \hat{a}_p n^p / p!}$ and estimate the remaining parameters, $\{A, a_0, a_1\}$, by the conventional single-tone parameter estimation algorithm.

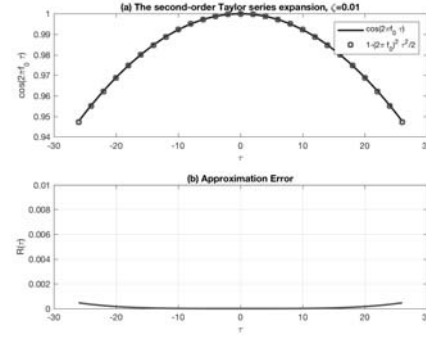


Fig. 2. The Taylor series expansion of (9). Top plot: the Taylor series expansion; Bottom plot: the approximation error over $|\tau| \leq 26$.

D. The Choice of ϵ

From the above discussion, it is clear that the Taylor series expansion in (9) is critical to the local HPF of (12). The number of samples included in the integration in (12) may be limited due to the local region ϵ is too small. On the other hand, ϵ cannot be arbitrarily large since the second-order Taylor expansion cannot hold. In the following, we use the remainder term of the Taylor series expansion to determine an upper bound of ϵ for a given approximation error. Define $z = 2\pi f_0$ and, hence, $f(z) = \cos(2\pi f_0 d_l \tau) = \cos(z) \approx 1 - \frac{z^2}{2}$. The remainder term $R(z) = f(z) - (1 - z^2/2)$ can be shown as $R(z) = \sin(z_c)z^3/6$ where z_c is a real number between 0 and z . As a result, we have $|R(z)| = |\sin(z_c)z^3/6| \leq |z|^3/6$. For a given upper bound ζ on the approximation error, the maximum local region ϵ can be determined as $|R(z)| \leq |z|^3/6 = \zeta \rightarrow |z| \leq (6\zeta)^{1/3}$ which is equivalent to

$$|\tau| \leq \epsilon = (6\zeta)^{1/3} / (2\pi d_{\max} f_{0,\max}) \quad (17)$$

where d_{\max} is the largest d_l and $f_{0,\max}$ is the upper limit on f_0 . As shown in Fig. 2, we compare $\cos(2\pi d_l f_0 \tau)$ with its Taylor expansion of (9) over $|\tau| \leq \epsilon = 26$. The local region is determined by using (17) with a bound $\zeta = 0.01$ and $2\pi d_{\max} f_{0,\max} = 0.015$. It is seen that the second-order Taylor expansion holds well and the approximation error (in the bottom plot) is well below the given bound at $\zeta = 0.01$.

E. Computational Complexity

We provide a brief comparison in terms of computational complexity. For the ML method, it requires $\mathcal{O}(N^{P+3})$ operations and the complexity is prohibitively high when the PPS order P is large. The PULS method requires $\mathcal{O}(N \log N)$ for the phase unwrapping step and $\mathcal{O}(N^2)$ for the one-time NLS fitting of (2) [22]. For the proposed LHPF method, it has similar complexity to the PULS method. The difference is that the proposed method uses $\mathcal{O}(\epsilon N \log \epsilon)$ operations to calculate the LHPF of (12) with the fast algorithm of [7], where $\epsilon < N$. The complexity of the HAF-based method is slightly higher than the PULS and LHPF methods as it takes $\mathcal{O}(N^2 \log N)$ operations to compute the HAF, followed by the one-time NLS fitting. Finally, with M window sizes, the QML method requires $\mathcal{O}(MN^2 \log N)$ operations for computing the STFT M times and $\mathcal{O}(MN^2)$ for implementing the NLS fittings M times [19]. The refining step further adds more operations. Therefore, the proposed method is computationally much lighter than the QML and ML methods.

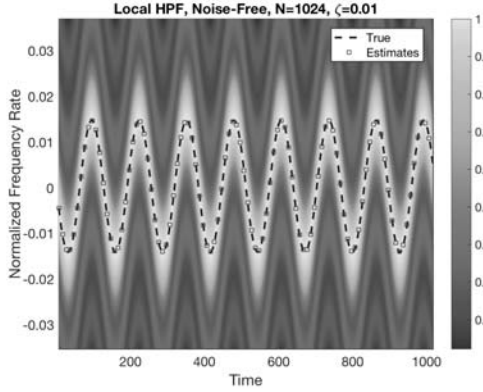


Fig. 3. The local HPF of the hybrid FM-PPS with $P = 2$ with $\omega_0 = 2\pi f_0 = 0.0491$, the same case as *Example 2* of [17].

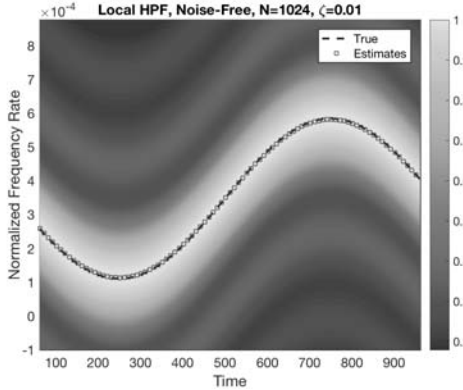


Fig. 4. The local HPF of the hybrid FM-PPS with $P = 2$ with $\omega_0 = 2\pi f_0 = 0.0063$, the same case as in Fig. 1 (b).

IV. PERFORMANCE EVALUATION

In this section, simulation results are provided to evaluate the proposed estimator. In the noisy scenario, the SNR is defined as $\text{SNR} = A^2/\sigma^2$.

A. Example 1: Hybrid Sinusoidal FM-PPS with $P = 2$

We first consider the noise-free case of Fig. 1 (a) with $\omega_0 = 2\pi f_0 = 0.0491$. Fig. 3 shows the local HPF (with $L = 1, d = 1, r = 1$) of the hybrid sinusoidal FM-PPS. We set the upper bound on the Taylor approximation error as $\zeta = 0.01$ which leads to the local region $\epsilon = 7$. As shown in Fig. 3, the true peak locations $\Psi(n)$, predicted by (12), are denoted by blue dash lines. The estimated peak locations $\hat{\Psi}(n)$, denoted by red squares, align well with the true peak locations. By using the detected peak locations,

TABLE I
MSE OF THE LOCAL HPF WITH $\zeta = 0.05$ IN EXAMPLE 2

SNR (dB)	MSE(\hat{b})	MSE($\hat{\omega}_0$)	MSE(\hat{a}_3)
10	$4.89 \cdot 10^{-6}$	$0.74 \cdot 10^{-8}$	$0.22 \cdot 10^{-18}$
15	$3.70 \cdot 10^{-6}$	$0.35 \cdot 10^{-8}$	$0.09 \cdot 10^{-18}$
20	$2.67 \cdot 10^{-6}$	$0.23 \cdot 10^{-8}$	$0.03 \cdot 10^{-18}$

TABLE II
MSE (SQUARED BIAS) OF THE HAF-BASED METHOD IN EXAMPLE 2

SNR (dB)	MSE(\hat{b})	MSE($\hat{\omega}_0$)	MSE(\hat{a}_3)
10	$8.73 \cdot 10^{-6}$	$6.00 \cdot 10^{-8}$	$12.56 \cdot 10^{-18}$
15	$5.99 \cdot 10^{-6}$	$2.84 \cdot 10^{-8}$	$14.81 \cdot 10^{-18}$
20	$5.75 \cdot 10^{-6}$	$2.82 \cdot 10^{-8}$	$14.76 \cdot 10^{-18}$

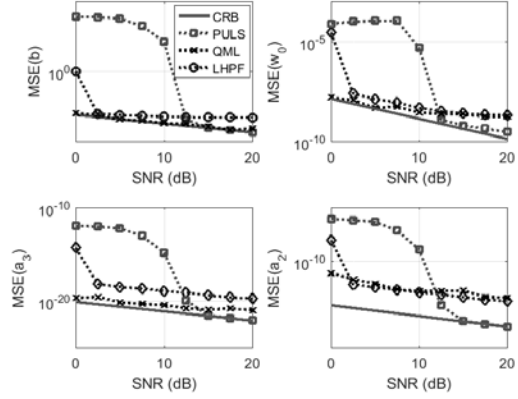


Fig. 5. The measured MSEs and CRBs for a hybrid FM-PPS with $P = 3$.

the phase parameters $\{a_2, b, f_0, \phi_0\}$ are correctly estimated from (14) and (16). Next, the sinusoidal FM frequency varies to $\omega_0 = 0.0063$, the same case as in Fig. 1 (b). Fig. 4 shows the local HPF of the hybrid sinusoidal FM-PPS. With $\zeta = 0.01$, the local region is increased to $\epsilon = 62$. It is seen that, compared with those in Fig. 3, the peak locations exhibit slower oscillation due to the smaller f_0 . Again, the detected peak locations match well with the true ones and, hence, the phase parameters are correctly estimated.

B. Example 2: Hybrid Sinusoidal FM-PPS with $P = 3$

We consider a hybrid FM-PPS with $P = 3$ which is also used in *Example 1* of [17]. With 500 Monte-Carlo runs, the measured mean square errors (MSEs) of the proposed estimator with $\zeta = 0.05$ are shown in Table I. For the HAF-based method, Table II shows the squared bias from Table I of [17]. Recall that the MSE is the sum of the squared bias and variance. As a result, the actual MSEs of the HAF-based method are larger than the number listed in Table II. Comparison between these two tables clearly shows that the proposed estimator has several orders of magnitude enhancements for these three parameters.

We also compare the measured MSEs of the proposed method with the PULS and QML methods as well as corresponding CRBs in Fig. 5. The performance of the PULS method reaches to the CRBs at high SNRs but becomes worse than the proposed LHPF estimator when SNR is below 12.5 dB. To efficiently evaluate the QML method, we use 6 window sizes $H = [4, 8, 16, 32, 48, 64]$ and choose the one yielding the largest likelihood function. Fig. 5 shows that the QML method gives lower MSEs for estimating b , ω_0 and a_3 but slightly higher MSEs for estimating a_2 . It appears that the window selection step of the QML method is not optimized for estimating a_2 .

V. CONCLUSION

In this paper, we proposed a local version of the HPF, originally designed for the pure PPS, for the hybrid sinusoidal FM-PPS. It shows significantly improved estimation performance than the HAF-based method. Compared with the PULS and QML methods, the proposed estimator offers a good trade-off between the estimation accuracy and computational complexity.

REFERENCES

- [1] S. Peleg and B. Porat, "Estimation and classification of signals with polynomial phase," *IEEE Transactions on Information Theory*, vol. 37, no. 2, pp. 422–430, 1991.
- [2] S. Shamsunder, G. B. Giannakis, and B. Friedlander, "Estimating random amplitude polynomial phase signals: A cyclostationary approach," *IEEE Trans. on Signal Processing*, vol. 43, no. 2, pp. 492–505, 1995.
- [3] S. Peleg and B. Friedlander, "The discrete polynomial-phase transform," *IEEE Trans. on Signal Processing*, vol. 43, no. 8, pp. 1901–1914, Aug. 1995.
- [4] S. Barbarossa and V. Petrone, "Analysis of polynomial-phase signals by the integrated generalized ambiguity function," *IEEE Trans. on Signal Processing*, vol. 45, no. 2, pp. 316–327, Feb. 1997.
- [5] S. Barbarossa, A. Scaglione, and G. B. Giannakis, "Product high-order ambiguity function for multicomponent polynomial-phase signal modeling," *IEEE Trans. on Signal Processing*, vol. 46, no. 3, 1998.
- [6] P. O'Shea, "A new technique for instantaneous frequency rate estimation," *IEEE Signal Processing Letters*, vol. 9, no. 8, pp. 251–252, Aug. 2002.
- [7] P. O'Shea, "A fast algorithm for estimating the parameters of a quadratic FM signal," *IEEE Trans. on Signal Processing*, vol. 52, no. 2, pp. 385–393, Feb. 2004.
- [8] M. Farquharson and P. O'Shea, "Extending the performance of the cubic phase function algorithm," *IEEE Trans. on Signal Processing*, vol. 55, no. 10, pp. 4767–4774, Oct. 2007.
- [9] P. Wang, I. Djurovic, and J. Yang, "Generalized high-order phase function for parameter estimation of polynomial phase signal," *IEEE Trans. on Signal Processing*, vol. 56, no. 7, pp. 3023–3028, July 2008.
- [10] P. Wang, H. Li, I. Djurović, and B. Himed, "Instantaneous frequency rate estimation for high-order polynomial-phase signals," *IEEE Signal Processing Letters*, vol. 16, no. 9, pp. 782–785, September 2009.
- [11] I. Djurovic, M. Simeunovic, S. Djukanovic, and P. Wang, "A hybrid CPF-HAF estimation of polynomial-phase signals: Detailed statistical analysis," *IEEE Trans. on Signal Processing*, vol. 60, no. 10, pp. 5010–5023, Oct. 2012.
- [12] S.-R. Huang, R. M. Lerner, and K. J. Parker, "On estimating the amplitude of harmonic vibration from the Doppler spectrum of reflected signals," *J. Acoust. Soc. Amer.*, vol. 88, pp. 2702–2712, Dec. 1990.
- [13] J.-E. Wilbur and R. J. McDonald, "Nonlinear analysis of cyclically correlated spectral spreading in modulated signals," *J. Acoust. Soc. Amer.*, vol. 92, pp. 219–230, July 1992.
- [14] M. R. Bell and R. A. Grubbs, "JEM modeling and measurement for radar target identification," *IEEE Trans. Aerosp. Electron. Syst.*, vol. 29, pp. 73–87, Jan. 1993.
- [15] S. Palumbo, S. Barbarossa, A. Farina, and M. R. Toma, "Classification techniques of radar signals backscattered by helicopter blades," in *Proceedings of Int. Symp. Digital Signal Process.*, London, UK, July 1996.
- [16] F. Gini and G. B. Giannakis, "Parameter estimation of hybrid hyperbolic FM and polynomial phase signals using the multi-lag high-order ambiguity function," in *Proceedings of The Thirty-First Asilomar Conference on Signals, Systems, and Computers*, Nov. 1997, vol. 1, pp. 250–254.
- [17] F. Gini and G. B. Giannakis, "Hybrid FM-polynomial phase signal modeling: Parameter estimation and Cramér-Rao bounds," *IEEE Trans. on Signal Processing*, vol. 47, no. 2, pp. 363–377, Feb. 1999.
- [18] S. M. Kay, *Modern Spectral Estimation: Theory and Application*, Prentice Hall, Englewood Cliffs, NJ, 1988.
- [19] I. Djurovic and L. J. Stankovic, "Quasi maximum likelihood estimator of polynomial phase signals," *IET Signal Processing*, vol. 13, no. 4, pp. 347–359, June 2014.
- [20] I. Djurovic, "QML-RANSAC: PPS and FM signals estimation in heavy noise environments," *Signal Processing*, vol. 130, pp. 142–151, Jan. 2017.
- [21] P. O'Shea, "On refining polynomial phase signal parameter estimates," *IEEE Trans. Aerosp. Electron. Syst.*, vol. 46, no. 3, pp. 978–987, July 2010.
- [22] G. Simon, R. Pintelon, L. Sujbert, and J. Schoukens, "An efficient nonlinear least square multisine fitting algorithm," *IEEE Trans. on Instrumentation and Measurement*, vol. 51, no. 4, pp. 750–755, August 2002.